

Characterization of Metal-Complex-Containing Organic Polymeric Films by Secondary Ion Mass Spectrometry

Nigel A. Surridge, Richard W. Linton,* Joseph T. Hupp, Scott R. Bryan, and Thomas J. Meyer

Chemistry Department, The University of North Carolina, Chapel Hill, North Carolina 27514

Dieter P. Griffis

Engineering Research Services Division, North Carolina State University, Raleigh, North Carolina 27695

The SIMS technique has been successfully applied as an analytical tool for the chemical and spatial analysis of metal-complex-doped polymeric films. The polymeric matrix was chlorosulfonated polystyrene (~1000 Å thick) cast onto a smooth platinum substrate, and following subsequent incorporation of metal complexes containing Ru, Re, or Zn by chemical binding, the SIMS technique was found to be chemically selective and sensitive to the Ru, Re, and Zn sites in the polymeric films. Qualitative assays of the films using secondary ion mass spectra were carried out with relative ease, but determinations of the spatial distribution of metal sites throughout the films require highly controlled sample preparation. The results of a series of studies on polymeric films containing various levels of the Ru complex showed that signals for Ru⁺ are influenced by local variations in ion yield, i.e., ion yield transients near the polymeric surface and at the polymer/platinum interface. A normalization procedure based on comparisons of Ru⁺ to O⁺ secondary ion intensities reduces the influence of such artifacts in the analysis of the concentration depth profiles of the complexes within the polymeric films.

Thin films ($\leq 1 \mu\text{m}$) of metal-complex-containing polymers on electrodes have been used for a number of ends (1) including chemical analysis (2), electrocatalysis (3-8), chemically based microelectronics (9), energy conversion (10-17), electrochromic displays (18, 19). Nonetheless, polymer-based coatings have remained, for the most part, poorly characterized, in part because the total quantity of coated material can be quite small even on large surface area electrodes. Typical coverages are 10^{-9} to 10^{-11} mol of monomeric units/cm², making analyses based on spectroscopic techniques such as infrared, Raman, or photoelectron difficult or impossible.

We report here an initial investigation where secondary ion mass spectrometry (SIMS) is used as an analytical tool for characterization of metallopolymeric films. We have examined the capabilities of the technique both for elemental analysis and the determination of metal content and for the ability of the technique to characterize distributions of the metal complex sites in the internal film structure using depth profiling studies. Experiments were carried out chiefly with thin films based on chlorosulfonated polystyrene (PS-SO₂Cl) deposited on platinum electrodes. Chlorosulfonated polystyrene appears to be an especially appropriate material for such an investigation. It is easily spun cast into thin films, is remarkably versatile as a reactive polymer (13, 24) (nearly 40 different organic and inorganic materials have been attached to PS-SO₂Cl films), and is of utility in photoelectrochemical (energy conversion) and electrocatalytic applications (12, 13, 25, 26).

EXPERIMENTAL SECTION

Materials. The metal complexes [Ru(bpy)₂(5-AP)](PF₆)₂ (bpy is 2,2'-bipyridine; 5-AP is 5-amino-1,10-phenanthroline), [Re(CO)₃(py)(5-AP)](PF₆) (py is pyridine), and *o*-aminotetraphenylporphyrinezinc (ZnTPP-NH₂) were available as preexisting samples (24, 27). Chlorosulfonated polystyrene (mol wt ~4000) was prepared as described previously (24). Tetraethylammonium perchlorate was prepared as described elsewhere (28). Acetonitrile was used as received from Burdick and Jackson, as was 2-butanone (99+%, from Aldrich).

Substrate and Film Preparation. Films were initially prepared by simple evaporative casting onto platinum foil from an acetone stock solution. While this procedure proved to be adequate for qualitative characterization, a more rigorous sample preparation protocol was required for quantitative work. Prerequisites of the sample substrate were that (1) it be extremely flat for surface analysis studies, (2) it be optically transparent for absorbance experiments in the visible region, and (3) an adhesive layer of platinum could be sputter deposited on the surface to act as an electrode for subsequent photochemical experiments (12, 13). Barium borosilicate glass satisfies these conditions and was chosen as a convenient substrate. Precut squares of the substrate glass (1.14 × 1.14 × 0.04 cm; Corning 7059 from F. G. Gray Co.) were subjected to a stream of high-pressure air to remove dust, rinsed with distilled water, transferred (without drying) to a 2-propanol solution, and sonicated for 30 min. The glass was then suspended above a second solution of 2-propanol (refluxing) for a minimum of 12 h and, after cooling and drying in the 2-propanol atmosphere, transferred rapidly to a Veeco VE 300 evaporator. The glass squares were then partially masked by an Al template, leaving uncovered a central section 4 mm in diameter together with a 2 mm wide strip along one edge and a connecting strip between the edge and center circle. This geometry for the electrode allowed illumination by light only at the central metal disk with connection of an electrical lead to the track along one edge during photochemical experiments. A 1000 Å thick film of Ti was then evaporatively deposited onto the unmasked portions of the glass to act as an anchor for the subsequent layer of Pt (~1000 Å), which renders the surface conductive. The Pt layer was deposited with a Polaron SEM E5100 sputter coater. At all stages of substrate preparation care was taken to minimize dust contamination.

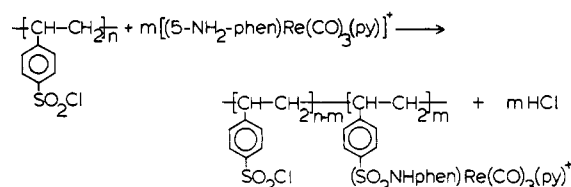
Polymeric films were cast by first dissolving a known quantity of PS-SO₂Cl in 2-butanone under inert-atmosphere conditions. A small amount of polymer solution (~10 μL) was then dropped onto a spinning slide (2000 rpm; Headway Research spin coater) and allowed to evaporate. By variation of the concentration of the polymer solution between 80 mM and 400 mM, film thicknesses were controlled between ~450 Å and ~3000 Å, although the most uniform film thicknesses were ≤ 1000 Å. All film thicknesses were measured using surface profilometry (Tencor Alpha-step 100 step profiler) and were found to vary by no more than $\pm 15\%$ when measured on various parts of the same sample. The reproducibility from one sample to another, using the same spin casting conditions, was $\pm 40\%$. The films were vacuum-dried at room temperature for 2 h. Exposure to air was minimized prior to metalation.

Polymer Film Metalation. Metal complex doping of the preformed film was achieved by soaking the assembly in 5 mM

Table I. Experimental Conditions for SIMS Studies

Primary Beam	
composition	$^{16}\text{O}_2^+$
accelerating potential	10 kV
impact energy	5.5 keV
diameter	50 μm
raster size	250 μm \times 250 μm
nominal current	100 na
Secondary Beam	
transfer optics	150 μm
field aperture	1.8 mm (mass spectra) 750 μm (depth profiles)
image field	150 μm (mass spectra) 60 μm (depth profiles)
contrast aperture	400 μm
energy offsets	-60 V (Zn spectra) -30 V (Ru depth profiles)

acetonitrile (Ru, Re complexes) or methylene chloride (Zn-TP-PNH₂) solutions of the appropriate metal complex. Metalation is based on sulfonamide formation between the -SO₂Cl sites in the precast film and amino substituents on the metal complex, e.g.



The attachment chemistry has been described in detail elsewhere (24). Varying degrees of metal complex incorporation were achieved for Ru by varying the soaking time from 2 min to 2 h to 20 h. Films for control experiments (blanks) were soaked in metal-free acetonitrile.

Following metalation each sample was soaked in 0.1 M tetraethylammonium perchlorate (TEAP)-acetonitrile for 30 min to remove entrapped (noncovalently bound) metal complex and then soaked in three successive clean acetonitrile solutions, each for 30 min, before drying and storing under vacuum. Failure to soak the films in clean acetonitrile resulted in TEAP microcrystallite formation upon drying and extensive film damage. For carefully treated films (as above), step profilometry indicated little change in the polymer-film surface morphology after chemical treatment.

A film was also prepared based on a premetalated soluble polymer. In a step preceding the spin casting, (bpy)₂Ru(5-AP)²⁺ was allowed to react with chloromethylated polystyrene, as described elsewhere (29), to achieve a loading of about 1% (i.e., the Ru complex was attached to ~1% of the R-CH₂-Cl sites). This polymer is homogeneous in Ru complex distribution. When dynamically evaporated from solution, it must necessarily produce a film that is also uniform in complex distribution.

Absorption Spectra. Visible spectra of films were obtained with the same type of glass substrate used for SIMS experiments. However, for the spectral experiments only a thin, semitransparent layer of platinum (~100 Å) was sputtered onto the glass surface and the entire glass square was coated. Films were then cast and treated following the steps outlined above. Transmission absorbance spectra of the resulting assemblies were obtained by use of an HP8450 diode array spectrometer.

Secondary Ion Mass Spectrometry (SIMS). A Cameca IMS-3f ion microscope equipped with a primary beam magnetic mass filter (30) was employed for the SIMS experiments. The microscope provides for stigmatic imaging via simultaneous detection of mass selected ions within the analytical image field. Mass spectra and depth profiles were obtained by using pulse-counting, electron multiplier detection. Multielement depth profiles were achieved via computer-controlled magnetic sector peak switching with 1 s counting times for each ion (¹²C⁺, ¹⁶O⁺, ¹⁰²Ru⁺, ¹⁹⁵Pt⁺) during each data acquisition cycle.

Typical operating parameters for the SIMS studies are summarized in Table I. A Faraday cup in the primary column was

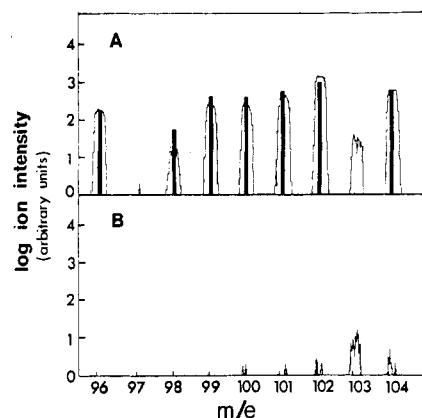


Figure 1. Secondary ion mass spectra in the Ru isotope range for PS-SO₂Cl film soaked in (A) 5 mM [(bpy)₂Ru(5-AP)] [PF₆]₂/acetonitrile and (B) acetonitrile. The solid bars indicate the natural abundance isotopic distribution for Ru.

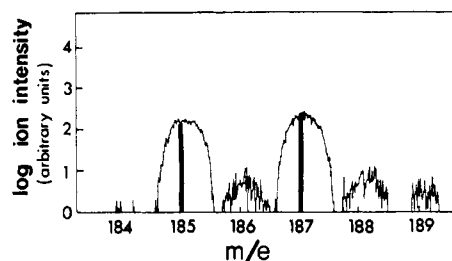


Figure 2. Secondary ion mass spectrum of PS-SO₂Cl film soaked in 5 mM (5-AP)Re(CO)₂Cl/acetonitrile. The solid bars indicate the natural abundance isotopic distribution for Re.

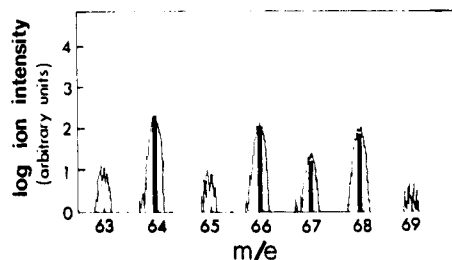


Figure 3. Secondary ion mass spectrum of PS-SO₂Cl film soaked in 5 mM ZnTPPNH₂/methylene chloride. The solid bars indicate natural abundance isotopic distribution for Zn.

used to estimate beam current. Appropriate secondary ion energy offsets (Table I) accompanied by energy slit translations for Zn⁺ and Ru⁺ measurements were necessary to remove possible polyatomic ion interferences.

RESULTS AND DISCUSSION

Qualitative Compositional Analysis. A series of initial SIMS experiments aimed at evaluation of detection capabilities for Ru, Re, and Zn in metal-doped polymeric films was performed. These metals are of particular interest since they are the central constituents of chromophoric complexes that have been incorporated in films and used to generate photocurrents (12, 13).

Shown in Figure 1A is a mass spectrum in the Ru isotope range for a Ru-doped film (2 min soak in Ru(bpy)₂(AP)²⁺). With the exception of *m/e* (mass-to-charge ratio) 103, which shows a significant intensity in control experiments on nonmetalated films (Figure 1B), there is a good correspondence between the observed distribution of ion intensities and that expected from natural Ru isotope abundances. The signal at *m/e* 103 is most logically assigned to a unidentified molecular fragment ion from the polymer (energy offsetting was not used in Figure 1).

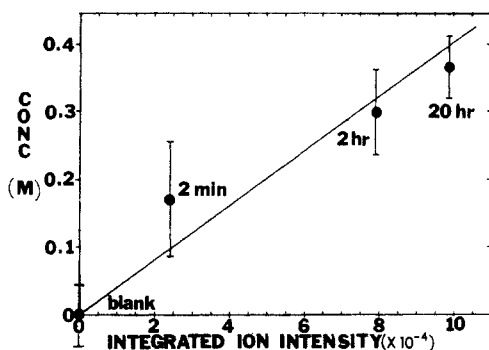


Figure 4. Concentration of Ru (in mol/L derived from film absorbances at 460 nm) vs. absolute secondary ion intensity for $^{102}\text{Ru}^+$ integrated over the entire depth of films. Shown are points for the blank film and films soaked for 2 min, 2 h, and 20 h in $[(\text{bpy})_2\text{Ru}(5\text{-AP})][\text{PF}_6]_2$ solution. (Error bars are 2σ for the variation in absorbance measured at various positions on the same polymeric film.)

Similar results were obtained with Re- and Zn-doped sulfonated polystyrene films as shown in Figures 2 and 3. In both cases there is evidence for the expected formation of small quantities of metal hydride species, e.g., m/e 65 or 69 for the most prominent Zn hydrides and m/e 186 or 188 for Re hydrides (note that ion intensities are plotted on log scales). An additional complication with the Zn-doped sample was the appearance of a significant interference at m/e 64 (possibly SO_2^+) which was removed by energy offsetting (Table I) to produce the result shown in Figure 3.

The available data clearly demonstrate that SIMS can be employed for the chemical analysis of metal complex dopants in organic films with good selectivity. From independent measurements based on film absorbances, the average Ru content of the polymeric film sample in Figure 1A is ca. 180 mM (equivalent to 7.1×10^{20} Ru atoms/cm³ of polymer film). The SIMS detection limit under the present analytical conditions is expected to be several orders of magnitude lower based on the intensity of the $^{102}\text{Ru}^+$ signal relative to a blank polymeric film sample. The SIMS sensitivity for the Re-doped film is similarly evident in that Re could not be detected by film absorbance experiments. Independent, qualitative evidence for the presence of Re is available, however, from photocurrent action spectra and from laser-induced luminescence (13).

Quantitative Compositional Analysis. Given the success of the preliminary qualitative measurements, the ability of SIMS to provide a quantitative measure of film doping was examined. A series of samples based on 0 min (blank), 2 min, 2 h, and 20 h Ru complex soaking times was prepared. Absorbance measurements at 460 nm (λ_{max} for $(\text{bpy})_2\text{Ru}(5\text{-AP})\text{-SO}_2\text{PS}$; $\epsilon(460) = 1.6 \times 10^4$) were used to quantitate the overall extent of Ru incorporation for each sample. A second series of films, identically treated but prepared on Pt/Ti/glass rather than semitransparent Pt/glass, was depth profiled using SIMS. The areas under the Ru^+ profiles were integrated between the polymeric surface and the Pt interface for each sample. In Figure 4 the resulting intensity sums are correlated with concentrations derived from absorbance measurements. A linear plot for the four data points is observed (correlation coefficient = 0.947). The longer soaking times produce the higher Ru concentrations, ranging from ~ 180 mM Ru (1.1×10^{20} Ru atoms/cm³ polymer) in the 2-min sample to ~ 380 mM Ru (2.3×10^{20} Ru atoms/cm³ polymer) in the 20-h sample. The low absorbance reading and corresponding poor precision for the concentration of the 2-min sample (Figure 4) indicate that Ru is close to the detection limit of the absorbance measurement for thin (~ 1000 Å) polymeric films. However, the SIMS count rate for the 2-min sample is still on the order of 1000 counts/s, i.e., about 3 orders of magnitude

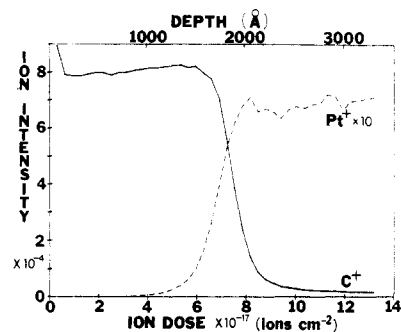


Figure 5. SIMS depth profile for $^{12}\text{C}^+$ and $^{195}\text{Pt}^+$ ions in PS- SO_2Cl film soaked for 20 h in $[(\text{bpy})_2\text{Ru}(5\text{-AP})][\text{PF}_6]_2$ solution.

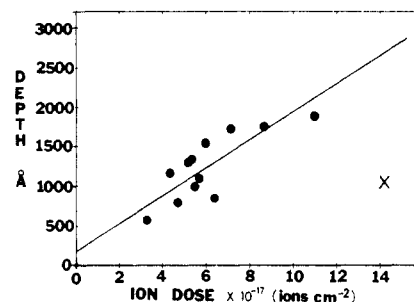


Figure 6. SIMS crater depth (as determined by step profiler) vs. primary ion dose (●, blank and Ru soaked PS- SO_2Cl films; X, PS- CH_2Cl film homogeneous in ruthenium).

above the detection limit. Due to the inherently large error included in measuring small absorbance values and the limited data set, the quantitative correlation of absorbance and SIMS measurements can be considered only as a preliminary finding.

A second aspect of quantitative film characterization relates to the depth resolution of SIMS measurements during polymeric film depth profiles. The location of the polymer/electrode interface was identified by monitoring both $^{195}\text{Pt}^+$ and $^{12}\text{C}^+$. With profilometry (Experimental Section), a polymer film thickness of 1750 Å was determined to correspond to the depth of the polymer/Pt electrode interface for the sample with SIMS profiles shown in Figure 5. The plot indicates that a primary ion dose (O_2^+) of the order of 8×10^{17} ions/cm² is required to sputter through the 1750-Å film. An operational definition of depth resolution is the depth required to reduce the C^+ intensity from 90% to 10% of its value in the polymeric film, or analogously, the depth required to increase the Pt^+ intensity from 10% to 90% of its value in the Pt substrate electrode. With this definition, depth resolutions achieved using either the C or Pt data in Figure 5 are ca. 360 Å, or about 20% of the sputtered depth. Contributing factors to depth resolution limitations are cascade mixing, nonuniform sputtering of the organic film (31), surface roughness of the Pt electrode, and nonuniform polymeric film thickness. In initial experiments using less rigorously prepared samples (i.e., evaporatively cast films on unpolished Pt foils), the interfacial resolution was significantly poorer. However, it is unclear whether the above values for depth resolution represent the limitation of the SIMS technique under the experimental conditions employed or whether depth resolution is limited by aspects of sample preparation.

A more extensive SIMS depth profiling study of Pt^+ and C^+ in various polymeric films is summarized in Figure 6. The average crater depths for several craters on each of five samples, measured by profilometry, are plotted against the approximate primary ion dose required to reach the polymer/Pt interface. The data for the chlorosulfonated polystyrene film soaked in the ruthenium complex for 0 min, 2 min, 2 h, and 20 h show a scattered but linear correlation as expected. The positive intercept of the regression line may reflect enhanced

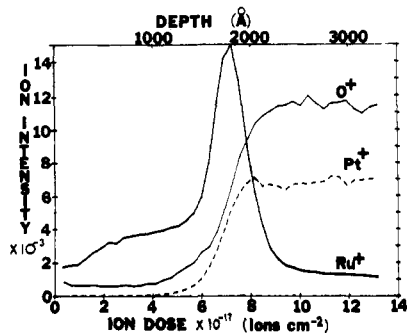


Figure 7. SIMS depth profile for $^{102}\text{Ru}^+$, $^{195}\text{Pt}^+$, and $^{16}\text{O}^+$ through a PS- SO_2Cl film soaked for 20 h in $[(\text{bpy})_2\text{Ru}(\text{5-AP})][\text{PF}_6]_2$ solution.

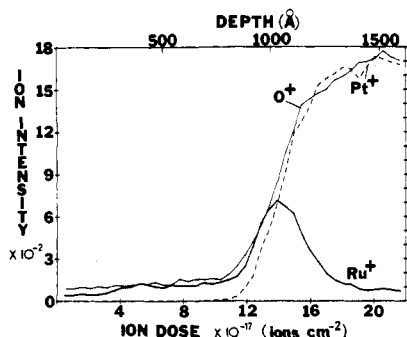


Figure 8. SIMS depth profile for $^{102}\text{Ru}^+$, $^{195}\text{Pt}^+$, and $^{16}\text{O}^+$ through a PS- CH_2Cl film homogeneous in $[(\text{bpy})_2\text{Ru}(\text{5-AP})][\text{PF}_6]_2$.

initial sputtering yields. This has been observed for other polymers (32) which exhibit declining sputtering yields as the polymer becomes increasingly carbonized by higher primary ion beam doses (31, 32). The data point for the chloromethylated polystyrene film lies significantly below the linear least-squares line for the chlorosulfonated polystyrenes indicating a lower sputter rate for this polymer. This may be due in part to the lack of oxygen as an elemental constituent of the polymer backbone, as well as differences in polymer density and molecular weight. The scatter in the data in Figure 6 reflects the uncertainty in assigning a position for the polymer/substrate interface from ion yield vs. primary ion dose plots. Nevertheless, it appears that the primary ion dose required to reach the interface provides a quantitative measure of relative film thickness within a particular type of polymer and that sputtering rates are highly sensitive to polymer composition.

Spatially Resolved Compositional Analysis. Of special significance in our photochemical experiments is the spatial distribution of chromophores through the polymeric films (13, 33). The possibility of detecting and measuring "concentration gradients" of metal complexes in films represented a primary motivation for investigating the SIMS technique. At first glance it would appear that the dopant spatial distribution could be straightforwardly measured by plotting the appropriate secondary ion intensity against sputtering time. Such a plot would represent a depth profile of dopant concentration through the polymer film.

Figure 7 shows a typical result using unprocessed SIMS data for a Ru-doped film. The profiles actually imply an increasing Ru concentration through the film with most of the Ru in the vicinity of the polymer/electrode interface. In order to investigate the validity of the depth profile, a *uniformly* metalated sample based on chloromethylated polystyrene was similarly depth profiled (Figure 8). Rather than generating a "flat" Ru^+ intensity throughout the polymeric film, the experiment yielded a plot similar in shape to that in Figure 7. This result is probably artifactual, and could be explained by an oxygen enhancement effect upon the ruthenium ion

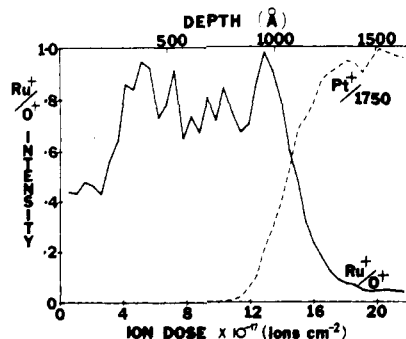


Figure 9. SIMS depth profile of $^{102}\text{Ru}^+/\text{O}^+$ ratio and $^{195}\text{Pt}^+$ through the homogeneous film, as in Figure 8.

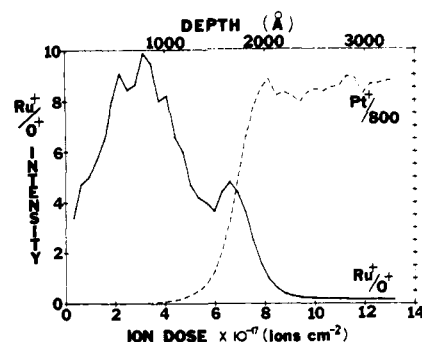


Figure 10. SIMS depth profile of $^{102}\text{Ru}^+/\text{O}^+$ ratio and $^{195}\text{Pt}^+$ through the film soaked for 20 h in $[(\text{bpy})_2\text{Ru}(\text{5-AP})][\text{PF}_6]_2$ solution, as in Figure 7.

yield if the local concentration of implanted oxygen were higher near the platinum interface. As the O^+ depth profiles indicate, the implanted oxygen is more concentrated in the Pt electrode relative to the polymeric film as the consequence of expected sputter yield differences between the two materials. As the sputtering approaches the Pt electrode, backscattering of the primary O_2^+ ions is expected to increase, since Pt has a much higher mass than the atomic constituents of the polymeric film (34). The effect is expected to result in an increase in the concentration of the implanted primary ion, and thus an enhanced Ru^+ ion yield, before the polymer/electrode interface is reached. In support of this, in all samples (e.g., Figures 7 and 8) the ion intensity data for $^{16}\text{O}^+$ secondary ions shows an order of magnitude increase near the polymer/electrode interface and is coincident with the maximum in the $^{102}\text{Ru}^+$ ion intensity.

In an attempt to correct for the interfacial ion-yield transient, the Ru^+/O^+ ion intensity ratio vs. ion dose was plotted in Figure 9 for the uniformly metalated sample. In the ratio plot the sample homogeneous in Ru shows, at least approximately, the expected flat Ru profile throughout the film. There are some inherent inaccuracies in this approach since the Ru^+ ion yield is likely to track nonlinearly with the implanted oxygen concentration. The point is also suggested in Figure 9 by (1) an initial small rise in the Ru^+/O^+ ratio until an apparent sputter equilibrium or steady-state condition is achieved at a depth of ca. 400 Å (as consistent with the estimated mean projected range of 5-keV O_2^+ ions in an organic matrix), and (2) a suggestion of a small peak in the Ru^+/O^+ ratio near the polymer/Pt interface. Future investigations will require much more detailed study of homogeneous films to establish more accurate, nonlinear corrections for these suspected ion yield transients. Such corrections would be comparable to those developed previously for specific inorganic matrices (35).

Application of the first-order correction suggested above to the *nonuniformly* metalated samples is shown by the Ru^+/O^+ plot in Figure 10 for the 20-h sample (uncorrected

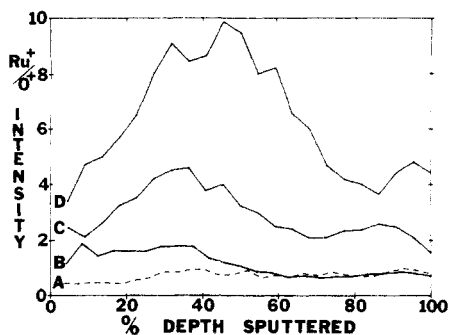


Figure 11. SIMS depth profiles of Ru^+/O^+ ratios for all polymeric films normalized for the various thicknesses: (A) film homogeneous in Ru; (B) film soaked for 2 min in Ru solution; (C) 2 h soak; (D) 20 h soak.

data previously shown in Figure 7). As for the case of the homogeneous film, the initial small rise in the Ru^+/O^+ ratio plot probably reflects the sputter depth needed to achieve a steady-state condition and is suspect due to ion yield transients. This transient may reflect the initial transformation of the polymer into a highly carbonized state by ion beam damage with concomitant changes in sputtering and secondary ion yields.

Figure 10 also shows a small local maximum for Ru^+/O^+ at the polymer/electrode interface. This suggests that the Ru^+ ion yield may increase more than the corresponding implanted oxygen concentration, as reflected by the O^+ secondary ion intensity, at the Pt interface. Thus, normalization to the O^+ intensity may somewhat undercompensate for the interfacial Ru^+ yield enhancement. It is possible that the secondary Ru^+/O^+ peak at the interface may also reflect enhanced Ru^+ signals resulting from (1) increasing sample electrical conductivity as the film becomes thinner and more carbonaceous due to primary ion beam damage (31), (2) preferential sputtering of low atomic number polymer constituents relative to Ru, (3) positive surface charging induced migration of Ru^+ to the Pt interface, and (4) inherent "pile-up" of Ru at the Pt interface during the soaking procedure via chemical reaction with surface oxides on Pt. The latter two mechanisms probably are insignificant because the Ru^+ is chemically bound to the polymer, and the extent of interfacial Ru binding to Pt is expected to be minimal. Preferential sputtering also does not appear to be a major factor since this would tend to gradually increase the Ru^+ signal through the polymer film rather than cause a local maximum at the polymer/electrode interface. It should be noted that apparent oxygen-enhancement and polymer/Pt interfacial effects also occur with the zinc- and rhenium-doped films. The raw data depth profile plots show dramatically enhanced metal ion intensities near the polymer/Pt interface.

A summary of the Ru^+/O^+ depth profiles, all plotted on the same intensity axis with a depth scale normalized to the total film thickness, is shown in Figure 11. All profiles peak at about 35% of the film thickness ($600 \pm 200 \text{ \AA}$) reflecting the approximate primary ion dose required to reach steady state conditions. It was expected that the maximum Ru loading should be in the outermost region of the film since the reactive Ru species was soaked into the film from an external solution. Indeed, the Ru^+/O^+ profiles for the three nonuniformly doped films (Figure 11B,C,D) indicate marked decreases in apparent Ru concentrations at depths greater than those estimated to reach steady-state sputtering conditions. As further evidence that these gradients are not a SIMS artifact, the depth profile for the uniformly doped film

shows no evidence of decreasing Ru concentration until the Pt interface is reached (Figure 11A, expanded plot shown in Figure 9). The profiles in Figure 11 also display the expected order of increasing Ru^+/O^+ ratios with increasing soaking time (Figures 11B,C,D); i.e., the amount of incorporated Ru in the polymer film increases with longer exposure to the solution containing the reactive Ru species.

LITERATURE CITED

- (1) Murray, R. W. In *Electroanalytical Chemistry*; Bard, A. J., Ed.; Marcel Dekker: New York, 1984; Vol. 13.
- (2) Guadalupe, A. R.; Abruna, H. D. *Anal. Chem.* **1985**, *57*, 142.
- (3) Samuels, G. J.; Meyer, T. J. *J. Am. Chem. Soc.* **1981**, *103*, 307.
- (4) Ellis, C. D.; Gilbert, J. A.; Murphy, W. R.; Meyer, T. J. *J. Am. Chem. Soc.* **1983**, *105*, 4842.
- (5) O'Toole, T.; Westmoreland, T. D.; Margerum, L. W.; Vining, W.; Murray, R. W.; Meyer, T. J. *J. Chem. Soc., Chem. Commun.* **1985**, 1416.
- (6) Martigny, P.; Anson, F. C. *J. Electroanal. Chem.* **1982**, *139*, 383.
- (7) Zak, J.; Kuwana, T. *Electroanal. Chem.* **1983**, *150*, 645.
- (8) Oyama, N.; Oki, N.; Ohno, H.; Ohnuki, Y.; Matsuda, H.; Tsuchida, E. *J. Phys. Chem.* **1983**, *87*, 3642.
- (9) Kittlesen, G. P.; White, H. S.; Wrighton, M. S. *J. Am. Chem. Soc.* **1984**, *106*, 5375, 7389.
- (10) Westmoreland, T. D.; Calvert, J. M.; Murray, R. W.; Meyer, T. J. *J. Chem. Soc., Chem. Commun.* **1983**, 65.
- (11) Calvert, J. M.; Caspar, J. V.; Binstead, R. A.; Westmoreland, T. D.; Meyer, T. J. *J. Am. Chem. Soc.* **1982**, *104*, 6872.
- (12) Hupp, J. T.; Otruba, J. P.; Parus, S. J.; Meyer, T. J. *J. Electroanal. Chem.* **1985**, *190*, 287.
- (13) Hupp, J. T.; Meyer, T. J., in preparation.
- (14) Oyama, N.; Yamaguchi, S.; Kaneko, M.; Yamada, A. *J. Electroanal. Chem.* **1982**, *139*, 215.
- (15) Oyama, N.; Yamaguchi, S.; Kaneko, M.; Yamada, A. *Makromol. Chem., Rapid Commun.* **1982**, *3*, 769.
- (16) Yamamura, T.; Umezawa, Y. *J. Chem. Soc., Dalton Trans.* **1982**, 1977.
- (17) Kaneko, M.; Oyama, N. *Electrochim. Acta* **1984**, *29*, 115.
- (18) Itaya, K.; Akahoshi, H.; Toshima, S. *J. Electrochem. Soc.* **1982**, *129*, 762.
- (19) Bookbinder, D. C.; Wrighton, M. S. *J. Electrochem. Soc.* **1983**, *130*, 1080.
- (20) Legg, K. D.; Ellis, A. B.; Bolts, J. M.; Wrighton, M. S. *Proc. Natl. Acad. Sci. U.S.A.* **1977**, *74*, 4116.
- (21) Bolts, J. M.; Bocarsly, A. B.; Palazzotto, M. C.; Walton, E. G.; Lewis, N. S.; Wrighton, M. S. *J. Am. Chem. Soc.* **1979**, *101*, 1378.
- (22) Bolts, J. M.; Wrighton, M. S. *J. Am. Chem. Soc.* **1979**, *101*, 6179.
- (23) Noufi, R.; Frank, A. J.; Nozik, A. J. *J. Am. Chem. Soc.* **1981**, *103*, 1849.
- (24) Ellis, C. D.; Meyer, T. J. *Inorg. Chem.* **1984**, *23*, 1748.
- (25) Vining, W. J.; Meyer, T. J. *J. Electroanal. Chem.*, in press.
- (26) Margerum, L. W.; Meyer, T. J., unpublished results.
- (27) Ellis, C. D.; Margerum, L. W.; Meyer, T. J.; Murray, R. W. *Inorg. Chem.* **1983**, *22*, 1407.
- (28) Sawyer, D. T.; Roberts, J. L., Jr., *Experimental Electrochemistry for Chemists*; Wiley: New York, 1974; p 212.
- (29) Margerum, L. W.; Murray, R. W.; Meyer, T. J., submitted for publication.
- (30) Blattner, R. J.; Evans, C. A. *Scanning Electron Microsc.* **1980**, *IV*, 55.
- (31) Simko, S. J.; Griffis, D. P.; Murray, R. W.; Linton, R. W. *Anal. Chem.* **1985**, *57*, 137.
- (32) Ullevig, D. M.; Evans, J. *Anal. Chem.* **1980**, *52*, 1467.
- (33) McClanahan, S.; Surridge, N. A.; Meyer, T. J., manuscript in preparation.
- (34) Williams, P.; Baker, J. E. *Nucl. Instrum. Methods* **1981**, *182/183*, 15.
- (35) Galuska, A. A.; Morrison, G. H. *Anal. Chem.* **1984**, *56*, 74.

RECEIVED for review March 4, 1986. Accepted June 3, 1986. Support for this work was supplied by the Army Research Office under Grant No. DAAG29-85-K-0121 and by the Department of Energy under Grant No. DE-AS05-78ER06034. Grant support for the Cameca IMS-3f ion microscope was provided in part by a grant from the National Science Foundation (DMR-8107499) and matching funds from the Microelectronics Center of North Carolina, North Carolina State University, and the University of North Carolina—Chapel Hill. The Cameca IMS-3f and digital imaging system are located at the Ion Microscope Facility operated by Analytical Services, Engineering Research Services Division, North Carolina State University.